HHS Public Access

Author manuscript

J Clin Neurophysiol. Author manuscript; available in PMC 2021 March 01.

Published in final edited form as:

J Clin Neurophysiol. 2020 March ; 37(2): 104–117. doi:10.1097/WNP.0000000000000488.

Therapeutic potentials of localized blood-brain barrier disruption by non-invasive transcranial focused ultrasound: A technical review

Amanda Cammalleri, B.A., **Phillip Croce, B.S.**, **Wonhye Lee, Ph.D.**, **Kyungho Yoon, Ph.D.**, **Seung-Schik Yoo, Ph.D., MBA**

Department of Radiology, Brigham and Women's Hospital, Harvard Medical School, Boston, MA

Abstract

The demands for region-specific, non-invasive therapies for neurological/psychiatric conditions are growing. We have witnessed the rise of transcranial focused ultrasound (tFUS) technology that temporarily and reversibly disrupts the blood-brain-barrier (BBB) in the brain with exceptional control over the spatial precisions and depth, all in a non-invasive manner. Starting with small animal studies about a decade ago, the technique is now being explored in non-human primates and humans for the assessment of its efficacy and safety. The ability to transfer exogenous/endogenous therapeutic agents, cells, and biomolecules across the BBB opens up new therapeutic avenues for various neurological conditions, with a possibility to modulate the excitability of regional brain function. In this review, we address the technical fundamentals, sonication parameters, experimental protocols, and monitoring techniques to examine the efficacy/safety in FUS-mediated BBB disruption, and discuss its potential translations to clinical use.

Keywords

Focused ultrasound; Blood-brain-barrier; Microbubbles; Contrast agent; Neuromodulation; Cavitation

1. Introduction

The blood-brain-barrier (BBB) plays an essential role in maintaining the normal physiology of the brain; however, it can complicate neurological treatment procedures by blocking the introduction of therapeutic agents and cells to the brain parenchyma. Advancement in transcranial focused ultrasound (tFUS) technique allows for the delivery of acoustic pressure waves to regional brain areas, with exquisite control over the size and depth. Research has shown that the pulsed application of the focused ultrasound (FUS), when combined with the intravenous (IV) injection of microbubbles (MBs) clinically used in ultrasound imaging, can temporarily and reversibly disrupt the regional BBB. This technique has shown new possibility for transferring exogenous pharmaceutical/biological agents across the BBB.

All the correspondence to: Seung-Schik Yoo, Ph.D., MBA yoo@bwh.harvard.edu Department of Radiology Brigham and Women's Hospital, Harvard Medical School 75 Francis Street Boston, MA 02115, USA TEL: 617-732-9464.

All authors declare that there is no conflict-of-interest.

This has opened up new avenues toward neurotherapeutic opportunities, yet the technique has many challenges ahead for its effective and safe use. In this review, we intend to provide the technical information regarding tFUS-MB mediated BBB disruption (BBBd) and its potential clinical translations based on a survey of the literature.

1.1. Brief review of structural and functional characteristics of the BBB

Extensive investigation has been performed to discover the roles and physiology of the BBB. The BBB serves as a physical barrier separating the blood circulating in the cerebral vasculature from the brain (1). The main function of the BBB is to protect the brain parenchyma from other foreign/immunogenic substances while allowing passive diffusional transport of water, lipid-/water-soluble gases, and molecules as well as facilitating active transport of key nutrients for neural function (2). It is distinguished from other types of barriers involving the brain, *e.g.*, the barrier existing between circulating blood and cerebrospinal fluid (CSF) (3).

The lumen of the cerebral vasculature in the brain is made up of cerebral endothelial cells that are ‘welded’ together by tight junctions. The extracellular domains of cells in tight junctions are composed of transmembrane proteins such as junctional adhesion molecules (JAM), occludins, and claudins. Neuronal cells such as pericytes and astrocytes are present around the cerebral vasculature, and play important roles in the proper formation and maintenance of the BBB. The normal function of the BBB is compromised mostly through trauma or sequelae from stroke. Abnormal function of the BBB has been implicated in neurological disorders such as epilepsy, demyelination diseases (*e.g.*, multiple sclerosis and amyotrophic sclerosis), psychiatric conditions such as schizophrenia, and neurodegenerative diseases such as Alzheimer’s disease (AD) (4–6).

1.2. Review of conventional methods to disrupt the BBB

Various means to modify the BBB permeability using solvents have been proposed (1), such as the administration of hyperosmotic solutions (7). These methods, with questionable safety, affect broad brain areas; therefore, targeted disruption is not possible. Localized temperature elevation achieved *via* microwave irradiation is known to disrupt the BBB (8). However, there are risks associated with thermal damage, which raise safety issues for its routine clinical use. Localized direct injection of drugs has been proposed (9), but it requires invasive procedures. Biological agents such as viruses or vasoactive molecules (*e.g.*, vascular endothelial growth factor) and compounds that utilize innate cell-mediated transport mechanisms have been used (10). These methods suffer from a lack of spatial specificity that would enable locally-targeted disruption of the BBB. A batch of ultrasound wave pulses, given at a moderate pressure-level, in a highly-repetitive fashion, also appear to disrupt the BBB (11).

1.3. Microbubble interactions with ultrasound

Mechanical pressure waves, including soundwaves, disrupt the integrity of the BBB. However, an excessive level of acoustic pressure is prone to damage targeted and surrounding brain tissues. This leads to investigations to find a way to deliver and amplify

the local acoustic pressure level just enough to disrupt the BBB without damaging the brain, and combined use of MBs with ultrasound was suggested (12).

The commercial introduction of various microbubble (MB)-based ultrasound contrast agents in the early and mid-1990s helped trigger the investigation of ultrasound-mediated BBBd. The MB was originally intended for enhancing echogenicity of the blood vessels by being confined in the vascular pool, for liver or vascular/cardiac ultrasound imaging, as contrast agents (CAs) (13). The size of the microsphere varies slightly, and there are several academic labs that develop in-house MBs with different sizes and material characteristics to be used as special delivery vehicles (14–17).

Although the detailed mechanism behind the FUS-mediated BBBd has yet to be ascertained, two major mechanisms have been suggested as likely candidates—one *via* stable cavitation (*i.e.*, wobbled expansion and contraction of MBs) and the other *via* inertial cavitation (extensive wobbles often resulting in ‘disrupting’ or ‘popping’ MBs). In more detail, stable cavitation involves harmonic, sub-/ultra-harmonic oscillations from MBs (15, 18–21), and becomes the dominant mechanism for BBBd when MB diameters are similar to the diameters of surrounding blood vessels (19). Inertial cavitation is caused by collapses and disruptions of MBs (causing broadband emissions) (15, 21), and can cause vascular damage (19, 20). When MB diameters are smaller than vessel diameters, inertial cavitation is more likely to occur (19, 22). These effects altogether amplify pressure waves experienced by the local blood vessels and can mechanically loosen adjacent endothelial barriers (23, 24).

2. FUS for the localized disruption of BBB – Basic fundamentals

Advancements in FUS techniques, with image-guidance for targeting the sonication focus to a specific region-of-interest, have enabled non-invasive delivery of highly-focused (with a focal size measuring a few millimeters) acoustic energy to biological tissues, by using acoustic lens (25), the geometric shape of the transducer (26), and the phased actuation of multiple FUS elements (27). The focused acoustic waves can deposit thermal and mechanical energy to a small, selected area of the human anatomy, and have been utilized for clinical applications ranging from thermal ablation to extracorporeal shock wave lithotripsy (28, 29).

Transcranial application of FUS, unlike sonication through soft tissue, casts many challenges, because the skull introduces significant aberration of the acoustic beam path *via* acoustic absorption/reflection/refractions. The use of a low fundamental frequency (typically < 1 MHz, which is much lower than the 1–15 MHz range used for clinical imaging) helps to alleviate concerns over the significant attenuation and refraction of the acoustic energy (30). The use of a phased-array FUS transducer configuration (consisting of > 1000 ultrasound elements surrounding the head) and the independent actuation of each transducer element, can further correct acoustic aberration caused by the skull (27, 31). These techniques have been utilized for thermal ablation of brain tumors and for functional neurosurgery in humans by adopting a high acoustic power (typically ranging from a few hundred to thousand watts) (32, 33). A single-element FUS transducer configuration, having a segmented spherical

shape with variable or fixed focal depth, is also used to deliver focused acoustic energy to the brain transcranially (34).

2.1. tFUS hardware

A few technical terms and hardware configurations to achieve successful BBBd are outlined. An MR-guided (MRg) clinical tFUS surgery platform, based on a helmet-style, multiple-element phased-array transducer configuration (*e.g.*, ExAblate™, Insightec, Israel), allows for the correction of phase aberrations (of the acoustic waves from each individual ultrasound transducer element) introduced by the skull by independently actuating the transducer elements that surround the human cranium (32, 33). The helmet is filled with circulating degassed water surrounding the head and a rubber diaphragm is used to block water leakage. The system is efficient in reaching deep brain areas, as the 'angle of attack' (noted as 'α'; in Fig. 1A) of the acoustic wavefront originating from each transducer element is large relative to the skull surface. However, when the focus is placed near the surface of the brain, such as cortical areas, the angle becomes smaller for a few transducers (noted as 'β'; in Fig. 1B), and subsequently increases the level of refraction/reflection at the skull surface beyond control. To remedy this shortcoming, beam-selection (selectively activating the arrays closest to the sonication target) or blocking of the waves that cause excessive aberration (illustrated in Fig. 1C) can be employed. These can also be substituted by the use of a smaller single-element FUS transducer (*e.g.*, Neurosona™, Neuro Science Network, LTD, Korea) having customizable focal size and depth) that is maneuvered around the skull under the image-guidance (illustrated in Fig. 1D).

Although it would be ideal to have the capability for electronic beam steering and focal size adjustment to provide ultimate flexibility in an experiment (achievable through the use of multi-arrayed transducers), a single-element configuration has been used in many exploratory BBBd experiments. A single-element transducer configuration, having a segmented spherical shape with variable or fixed focal depth, grants the (practical) wearable design for both humans and large animals. The sonication location can be changed by moving the transducer around the scalp while acoustic coupling media, such as a (degassed) water-filled bag (35) or a compressible polyvinyl alcohol hydrogel (36, 37), are provided at the interface. The utility of a single-element design was already demonstrated in delivering highly-focused acoustic energy across various brain areas in sheep as well as in humans (11, 34).

2.2. Image-guidance

To visualize acoustic wave propagation and focal location, MRI-based thermometry imaging (35) or Acoustic Radiation Force Imaging (AFRI) (38) have been proposed; however, heating of the brain tissue may not be a desirable option in many clinical cases while the sensitivity of ARFI is not sufficient to detect elastic changes of the brain tissue at the acoustic focus. Therefore, image-guidance is desired to inform the operator of the location of the focus in the brain. To do so, neuroanatomical information (through magnetic resonance imaging; MRI and computed tomography; CT) is acquired from the individual, and this 'virtual' information is registered to the actual space of the individual's head (38). By subsequently tracking the relative spatial and orientation information of the transducer

with respect to the head in real-time using optical tracking systems, one can reasonably estimate the location of the focus. However, due to the attenuation and deviation of the wave propagation through the skull, simple geometric/spatial information of the focus based on transducer specifications may not be sufficient to accurately predict the location, shape, and intensity of the focus. To augment the accuracy of image-guidance and to predict the state of the acoustic wave propagation through the media, (especially the *in situ* acoustic pressure at the focus), a computer-based numerical simulation can be used (39, 40). The simulation-assisted guidance not only increases the spatial accuracy of sonication, but also informs the operator of potential safety risks, such as the formation of standing waves (41) that can create unwanted acoustic foci in the brain.

2.3. Pulsing schemes of tFUS for BBBd

Continuous application of FUS energy to a local brain area can eventually elevate the tissue temperature when given beyond a level at which the generated heat will not dissipate quickly. To disrupt the BBB without heating the brain tissue, tFUS is typically given in a batch of pulsed applications of ultrasound pressure waves (illustrated in Fig. 2) at fundamental frequencies (FF), typically in a range of 200–700 kHz. The batch of bursts of pulses, each having a specific tone-burst-duration (TBD), are administered in a repeated fashion with a pulse repetition frequency (PRF), whereby TBD and PRF together determine the duty cycle (DC) of sonication (in %, which indicates the fraction of active sonication time). Since the PRF is low in BBBd, on the order of 0.5–2 Hz (see later section), the nomenclature of DC is seldom used. The overall duration of pulsed sonication is termed as sonication duration (SD).

FF is inversely related to wavelength (speed of sound in the water ÷ FF). Therefore, increasing the FF reduces the wavelength. Assuming the sound of speed in the water/biological tissue is estimated to be around 1500 m/s, the wavelength of the ultrasound at 250 kHz, for example, would be 1500 m/s ÷ 250 kHz = 6 mm.

It is important to note that the wavelength is one of the key elements to determine the rate of transmission through the skull, whereby the use of longer wavelengths (*i.e.*, smaller FF) generally results in better acoustic transmission through the skull. For example, in the case of the human skull, at FF > 1 MHz, most of the acoustic energy (> 99%) is lost and cannot be transmitted through the cranium. The wavelength, on the other hand, limits the minimum achievable size of the focus (in diameter and length; the focus is generally ellipsoid in shape with its long axis aligned to the sonication direction). Although the size and shape of the focus is dependent on many factors, such as transducer geometry and configurations (described further in Section 2.4 below), the use of a shorter wavelength generally improves the overall spatial selectivity of the sonication (by generating a smaller focus) while a longer wavelength reduces spatial selectivity (by generating a larger focal size). Therefore, compromise must be made between the transmission rate and the size of the focus.

The energy of the acoustic waves is also an important parameter in the FUS application, and is typically represented by acoustic intensity, *i.e.*, the acoustic power per given area (*i.e.*, W/cm^2). Acoustic intensity is conventionally expressed in spatial-peak pulse-average intensity (I_{sppa}) while spatial-peak temporal-average intensity (I_{spta}) represents its time-

averaged value per stimulus. The nomenclature, however, is not favorably used in the field of FUS-mediated BBBd since the effectiveness of disruption is related to the acoustic pressure at the focus (represented in unit, Pascal; Pa). The mechanical pressure waves have positive (*i.e.*, 'push') and negative (*i.e.*, 'pull') components in an oscillating manner in the time domain. Only unidirectional amplitude, particularly negative peak pressure (represented as the peak rarefactional pressure) is considered important for estimating the effectiveness and safety of the method.

Another component to be considered is Mechanical Index (MI), which is a generally-accepted index to gauge the safety of the ultrasound output. MI is a unit-less index that involves both FF and pressure, and is defined as peak rarefactional pressure (in MPa) ÷ √FF (in MHz). A higher MI is associated with higher risks of mechanically affecting the biological tissue. In the context of tFUS-MB mediated BBBd, McDannold and colleagues have found that MI is positively correlated with efficacy of BBBd (42). Some literature started to introduce a new index called Cavitation Index (CI), peak rarefactional pressure (in MPa unit) ÷ FF (in MHz unit), to gauge the efficacy of the BBBd and the likelihood of subharmonic emissions from stable cavitation (18, 20). However, this model is limited to a relatively high frequency range (> 800 kHz), and may not be used in the FF range applicable for use in humans (18).

2.4. Parameters that affect the focal shape and size of tFUS

In addition to FF (and associated wavelength), the spatial selectivity of the FUS, *i.e.*, 3-dimensional acoustic pressure distribution generated by the FUS transducer, is profoundly influenced by multiple factors such as transducer type/geometry (*e.g.*, segmented sphere or lens-mediated focusing) and its configurations (*e.g.*, single-element or multiple array) (43). Therefore, the wavelength of the ultrasound alone cannot reliably predict the volume/shape of the affected tissues. In the case of a single-element transducer, the 'tightness' of the focus is often related to the 'F-number' (f_n) of the transducer (the depth of the focus divided by the width of transducer aperture). A large f_n (in which the depth of the focus is much greater than the transducer aperture) tends to create an elongated focus. On the other hand, an excessively small f_n (< 0.5, the focal depth is much smaller than the transducer aperture) not only limits the depth penetration but also can create a small 'angle of attack' that subsequently increases the level of refraction/reflection at the skull surface (illustrated in Fig. 1B). Therefore, an f_n of ~1 (a width of a transducer aperture close to the focal depth) is favored for FUS applications. For example, a single-element, acoustic lens-based FUS transducer (Neurosona™, Neuro Science Network, LTD, Korea) having the f_n = 1.2 (30 mm aperture and 37 mm focal depth from the exit plane of the transducer) and FF=250 kHz shows the ellipsoidal pressure distribution with 3 mm diameter (along the short axis) and 17 mm along the long axis measured at 90% maximum pressure level (Fig. 3).

Furthermore, the acoustic pressure waves interact with the skull and underlying brain tissues *via* linear and non-linear absorption/scattering/reflections that inevitably affect the shape/size/intensity of the acoustic focus, which warrants the use of a computer-based numerical simulation for its characterization. The detailed theoretical foundations that dictate

ultrasound parameters to the resulting shape of the acoustic focus *in situ* are discussed elsewhere (41, 44).

3. In-depth technical overview of FUS-mediated BBBd

With this background information, more detailed aspects of FUS-mediated BBBd are introduced herein.

3.1. Used hardware type for the tFUS

Custom-made tFUS systems, mostly based on single-element segmented spherical transducers, have been extensively used (40, 42, 45, 46) while clinical-grade, multi-arrayed FUS systems have also been deployed (47). Single-element transducers, with variable focal lengths, can be used to sonicate specific brain regions by adjusting the location and orientation of the transducer along the scalp. Arrayed transducers can accurately sonicate deeper brain regions due to their ability to correct aberrations from the skull bone. The FUS transducers can be prepared with cavitation detectors, mounted in water on each side of the transducer head (47) or placed coaxially and confocally within a transducer (14, 15), for real-time monitoring of acoustic emissions. Cavitation detection can be separately conducted from an agar-based vessel phantom to assess cavitation at varying pressures (20). The use of hydrophones (*e.g.*, Y-107, Sonic Concepts™, WA, USA) that 'listen' to the subharmonic emissions of the MB activity from the brain can provide feedback to the operator to adjust the *in situ* acoustic pressure, which can vary depending on the individual skull geometry or differences in vasculature diameter (15).

3.2. Ultrasound contrast agents

Although there are new MBs being introduced to the market with novel capabilities, three major MBs have been approved for clinical use (availability and market approval varies depending on country). Definity™ (Lantheus Medical Imaging, North Billerica, MA, USA) consists of perflutren lipid microspheres (mean diameter of 1.1–3.3 μm with a maximum diameter of 20 μm). SonoVue™ (Bracco Imaging, Milan, Italy) is the suspension of phospholipids microsphere containing sulfur hexafluoride gas (mean diameter of ~2.5 μm; more than 90% of the bubbles are smaller than 8 μm). Optison™ (GE Healthcare, Princeton, NJ, USA) consists of sterile non-pyrogenic suspension of microspheres of human serum albumin with perflutren (mean diameter of 3.0–4.5 μm with a maximum diameter of 32 μm). These MBs are typically injected intravenously (IV) and temporarily stay in the vascular space until they are eliminated from the body (with different half-lives; Definity™: ~1.3 min; SonoVue ™: ~12 min; Optison™: ~10 min). Half-life varies depending on the chemical composition, size, and charge characteristics of the MBs.

MB size and dose of administration during FUS application have been reported to positively correlate with degrees of BBBd. Hosseinka *et al.* found that vascular wall stresses are dependent on bubble size, supporting the statement that MB-induced mechanical stresses influence BBBd (23). The amount of MB at the site during the sonication, therefore, affects the degree of BBBd, *i.e.*, higher MB concentration increases the probability of BBBd in any

given time period (46). However, for human applications, the maximum dose (*via* bolus IV or continuous injection) is limited clinically.

Regarding the timing of the MB introduction with respect to the timing of the sonication, many studies have employed a preemptive IV injection of MBs in a bolus fashion, immediately followed by the sonication; however, some studies have used either (1) continuous injection of the MBs (48) or (2) sonication accompanied or followed by bolus injection of the MBs (14–16). O'Reilly et al. found no significant difference between the bolus administration (15 s) and longer infusions of the MBs in the efficacy of BBBd (49).

3.3. Focused ultrasound parameters affecting the efficacy of BBBd

The effects of FUS parameters, *i.e.*, (1) TBD, (2) PRF, (3) SD, (4) FF, and (5) *in situ* acoustic pressure, on BBBd are described in more detail.

Tone burst duration (TBD) and Pulse repetition frequency (PRF)—As the length of time for each burst of sound waves (*i.e.*, TBD) increases from 0.1–10 ms, the extent of BBBd also increases (50), however, these effects start to plateau for bursts over 10 ms. This may be because MBs near the focal region are destroyed at a higher TBD, thereby requiring a reperfusion of MBs into the corresponding vasculature (1, 50).

The optimal PRF for BBBd is likely to be 1 Hz. O'Reilly et al. have shown that PRF below 1 Hz did not sufficiently yield the T1-weighted MRI signal enhancement associated with BBBd, whereas, a PRF of 2 Hz only slightly increased enhancement (49). McDannold *et al.* tested PRFs from 0.5–5 Hz, and found the greatest mean signal intensity enhancement (from contrast enhanced T1-weighted MRI) at 1 Hz (50). Based on these findings, many studies have used PRFs of 1–2 Hz (14, 17, 19, 45, 46, 48, 51–64).

Sonication duration (SD)—The time period of the entire FUS sonication has been found to positively correlate with BBBd from 0–40 s and then plateau from 40 to 60 s (58). FUS exposure time over 300 s has been shown to cause tissue damage (1). This is congruent with a recent study on large animals (sheep) whereby the excessively repeated (a few hundreds of FUS sonication events) sonication with relatively short time intervals (*i.e.*, 300 ms), even without the presence of MBs, resulted in minor microhemorrhaging (without edema) (11). Although a duration of 1–2 min has been favored by many FUS-BBBd studies, it is likely that an SD exceeding 2 min can also be used in conjunction with proper monitoring methods such as cavitation detection and dynamic contrast-enhanced MRI (described below).

Fundamental frequency (FF), In situ acoustic pressure, and Mechanical index (MI)—Fundamental frequency (FF) has been shown to affect BBBd. Higher frequencies require greater pressure amplitudes to open the BBB. This phenomenon has been previously shown in various rabbit and rodent studies using FFs ranging from 260–1700 kHz (45, 46, 48, 49, 51, 53–60, 63, 65, 66). Although not performed transcranially, implantable transducers have recently been tested in non-human primates (NHP) and humans to avoid attenuation from the skull bone (62, 64, 67). These studies utilizing intracranial transducers have shown BBBd without hemorrhaging or tissue damage with a FF of 1050 kHz (62, 67). In the context of transcranial transmission, due to a thicker skull bone in humans (on the

order of 5–7 mm, but varying depending on location and the individual), transcranial FUS would require a lower FF for BBBd. Therefore, compromise has to be made in determining the FF to balance the rate of acoustic transmission and the minimum size of the focus. Typically 200–700 kHz seems to be an appropriate choice for the transcranial FUS in humans.

Acoustic pressure level is another crucial factor in determining the level of BBBd. As introduced in the previous section, higher pressure would increase the level of cavitation of MBs, and therefore, increase the probability of BBBd, but with a greater risk for brain tissue damage. It is important to note that, at the same pressure level, the use of a lower FF would increase the MI (see section above for the definition of MI), which could result in non-reversible tissue damage/bleeding.

Although there is not an absolute consensus, MI became the factor to estimate the degree of BBBd as well as potentials for tissue damage. Greater MI increases the probability of successful BBBd, but also increases the extent of hemorrhaging and tissue damage (42). McDannold *et al.* found that the BBBd threshold, where the probability for disruption is 50%, occurs at an MI of 0.46, which remained the same for different frequencies tested (42). To survey the relationship among FF and acoustic pressure (with corresponding MI values), we compiled results from 14 studies that evaluated the presence/extent of damage across various FF (under 1 MHz) and acoustic pressures (Fig. 4). A more comprehensive overview of existing studies over a wider range of FF, along with different experimental parameters and study designs, is given in Table 1.

According to the compilation, a minimum MI of 0.3 is necessary to elicit BBBd, while up to 0.7 can be used without inducing apparent hemorrhaging or tissue damage. It is notable, however, that minor damage (*i.e.*, few extravasated blood cells) was observed at an MI of 0.3 performed at 560 kHz among rats (56) as well as from another study conducted among rabbits using an MI of 0.5 at 690 kHz (50). It is important to note that many of these studies were done transcranially on smaller animals whereby the possibility of having acoustic reverberation is high (68). More recent studies, using intracranial FUS technology (delivered through implanted FUS transducer) on NHP and humans, showed that BBBd can be achieved without damage at MIs of 0.8–1.12 (62, 67). As MI may not be a sole factor in gauging the effectiveness/safety of the technique, further studies are needed.

3.4. Methods to visualize/characterize the blood-brain barrier disruption

Various techniques have been used to characterize BBBd. In animal models, Evan's blue dye (or trypan blue) can be injected during cardiac perfusion that fixates the brain tissue. These dyes leak out from the disrupted BBB into the brain parenchyma and are evaluated histologically (47, 52, 54, 57, 58, 60). Injection of fluorescent tagged dextrans has been used for visualization of BBBd (65). Electron-microscopic images (TEM) were also used to assess the degrees of BBBd (40). However, these techniques are not compatible with clinical use in humans.

MRI, as a non-ionizing imaging modality, has been extensively used to evaluate the degrees of BBBd as well as to assess the presence of hemorrhaging. Gadolinium (Gd)-based MR

CAs such as Magnevist™ (Gadopentetate Dimeglumine, Bayer Healthcare, Whippany, NJ, USA), Omniscan™ (Gadodiamide, GE Healthcare, Princeton, NJ, USA), or OptiMARK™ (Gadoversetamide, Guerbet Co, Villepinte, France), are injected through IV after the BBBd. These agents, due to their small size, leak out from the vascular space through the disrupted BBB, and enhance T1-weigted MR signals. The MR images before and after BBBd are compared, and the areas showing signal enhancement (often quantified in percentage signal increase from the baseline image) indicate regions where successful BBBd occurred.

Excessive BBBd can result in local hemorrhaging and local accumulation of hemosiderin, and, therefore, must be monitored/evaluated during/after the procedure. Iron contents associated with hemorrhaging shorten the T2* constant of the affected brain tissue, reducing T2*-weighted signals. Susceptibility weighted imaging (SWI), typically using a long TE (Time of Echo) during the gradient-echo MR acquisition, is deployed to detect these regions by taking images before and after the BBBd procedure (52). For these reasons, the use of iron-based cell-labeling (such as superparamagnetic iron oxide; SPIO) to assess the amount of cells delivered by the FUS-BBBd procedure (40), should be carefully evaluated to distinguish the iron contents for labeling from hemorrhaging. A dual contrast mechanism, utilizing echo-time shifted SWIs, can be gainfully adopted to reduce this confounder (69).

We note that simple comparisons (*i.e.*, image subtraction) of contrast-enhanced (*via* MR contrast agents) T1-weighted images before and after the BBBd procedure, may not have sufficient sensitivity. This is especially true when low acoustic pressure waves are applied to minimally disrupt the BBB, reducing the T1-signal contrast at the site of disruption. Therefore, time course of the contrast enhancement, with the aim of accounting for the pharmacokinetics of Gd-enhancement, recently started to take place for the visualization and quantification of the BBBd. This technique, referred to as Dynamic Contrast Enhanced MRI (DCE-MRI), traditionally utilized in malignancy detection of tumors and assessment of stroke, can be used to measure the transfer coefficient for gadolinium (K_{trans}) (70, 71). When applied to quantify the degree of BBBd, DCE-MRI identified that increases in acoustic pressure elevated the K_{trans} value, supporting the correlation of applied pressure to the degree of BBBd (20). This technique inherently has a higher sensitivity in the assessment of BBBd compared to the simple image-subtraction, which may reveal the effectiveness of safer parameters, and is recommended to be used in a clinical setting. The use of an automated data processing technique, such as independent component analysis (ICA) (70), can be adopted to analyze the MR signal enhancement patterns.

3.5. Duration of blood-brain barrier disruption and Spatial extent

BBBd from tFUS-MB administration is transient and reversible. Detailed information regarding the duration of the BBB opening is necessary. The contrast-enhanced T1-weighted MRI signal immediately reached its maximum following the administration of FUS, and decreased over time (45), suggesting that BBBd is achieved almost immediately after FUS. The BBB opening has been shown to be near complete closure 5 hours after sonication with no evidence of BBBd after 4–5 weeks (51). An additional imaging study has shown the BBB to be completely closed after 2–5 days (45, 72) suggesting that the disruption can far outlast the duration of the sonication itself. The duration of BBBd is dependent upon the choice of

acoustic parameters and the choice of MB agents. Further studies are needed to identify their detailed correlations.

The spatial extent of BBBd can vary depending on the spatial distribution of peak negative pressure. BBBd volume increased proportionally with *in situ* pressure level (16). At a constant pressure (*e.g.*, at 0.4 MPa), varying degrees of incidence sonication angle with respect to the skull surface altered the *in situ* profile of the acoustic focus as well as the volume of subsequent BBBd (16). FUS sonication, and concurrent disruption of the BBB, can be patterned in multiple locations, and overlapped in the same location multiple times. For example, FUS has been used to disrupt the BBB around the following target areas in animal models through multiple sonication events that occurred in one experimental session —bilateral targets in hippocampus and LGN, primary visual cortex, cingulate cortex and amygdala (47); thalamus, putamen, cingulate cortex, visual cortex, hippocampus, white matter structures, and LGN (hippocampus and optic tract) (47); thalamus, hippocampus, superior colliculus, caudate, and putamen (46).

3.6. Used animal species and Anesthetic agents

Previous studies have administered FUS for BBBd on rabbits (42, 45, 50, 51) and rodents (46, 52–56, 58, 65), and, more recently, NHP, such as macaques (14, 16, 17, 19, 47, 67) and baboons (62, 67). Animal choice is important, because the safest and most effective FUS parameters may differ depending on animal species. Brain size and skull thickness, along with a varying vasculature in different animals, can affect MB cavitation and BBBd differently. For example, smaller blood vessels (10–30 μm) are more susceptible to the BBBd procedure than larger vessels (20–70 μm) (73), thereby requiring a lower acoustic intensity for BBBd. Changes in vascular parameters like blood flow, blood pressure, and blood vessel dilation/constriction are also known to affect MB activity and interactions with ultrasound waves (57).

Most small animal studies were done under anesthetic conditions, such as ketamine/xylazine, and isoflurane. In NHP, similar anesthetic agents have been used (16). However, it is important to acknowledge that anesthetic agent and dose affect vascular factors and have shown to influence BBBd. McDannold *et al.* found that rats anesthetized with a cocktail of ketamine and xylazine showed greater BBBd enhancement with contrast-enhanced MRI than rats anesthetized with isoflurane and oxygen (57). Few NHP studies are reported in the absence of anesthetic agent (14, 62, 67). The ability to perform FUS-mediated BBBd sessions on awake animals/human subjects is desired not only to eliminate the confounding effects from anesthesia but also to be able to monitor the behavioral responses.

3.7. Safety considerations

Heating of the skull in the path of sonication may occur during the application of high-intensity FUS (HIFU); however, is not likely in FUS-mediated BBBd procedures due to the use of low acoustic energy. Rather, damages may occur at the site of BBBd and/or the surrounding tissues. The types of potential damages include hemorrhaging, ischemia, cell membrane disruption, and possibly a sterile inflammatory response (SIR). Rodent studies have previously observed hemorrhaging after tFUS-MB administration at pressure

amplitudes of 0.8 MPa or higher (52, 54, 61, 63, 65). A recent study by Kovacs *et al.* found genetic level changes in heat-shock protein 70, IL-1, IL-18, and TNFα at the sonicated site (mimicking a SIR) after tFUS-BBBd treatment at 590 kHz, using 0.9 MPa pressure waves (48). It is important to note that these effects were found in mice and were only examined for a 24 h period. Also, due to the use of a higher MI in the study (*i.e.*, 1.2) which is prone to damage the brain tissue, further study is warranted to evaluate the presence of similar inflammatory responses using a lower pressure level (and lower MI).

The safety of repeated tFUS-MB administration to the same locations needs to be assessed for potential clinical translation of the method that requires multiple treatments. Recent studies on NHPs have shown promising results. For example, repeated exposure to the sonication from the implanted FUS device every 15 days over a 4-month period among baboons and a macaque resulted in no behavioral consequences, no epileptic signs or pathological central nerve conduction, and resulted in detection of only a few erythrocytes at the sonication site upon histological examination (67). Downs and colleagues applied multiple BBBd sessions on the caudate, putamen, and thalamus of awake macaques performing visuomotor control and motivation tasks, and found no edema or microhemorrhage from the brain (14). In addition, no negative physiological or neurological effects were detected from repeatedly opening the BBB around the basal ganglia across the 20-month testing period in macaques (14). Likewise, repeated tFUS-MB (*i.e.*, five sessions over 5–9 week period) for BBBd in the central visual field targets of macaques did not affect their behavior or performance on visual acuity tasks (47). It is, however, important to note that MBs were made in-house in some of these studies which may have affected the safety parameters.

Repeated FUS-mediated BBBd sessions were also administered in a clinical study using an intracranially implanted FUS transducer to enhance a local delivery of carboplatin for patients with recurrent glioblastoma (62). Patients, who were alert during the procedure, were exposed to up to four sets of BBBd sessions (FF = 1050 kHz, TBD = 23.8 ms, SD = 150 s, PRF = 1 Hz, Pressure = 0.8–1.1 MPa) and showed no damage or behavioral changes from the procedure. Pressures of 0.5 MPa and 0.65 MPa were also administered safely in this study, but did not induce BBBd, based on contrast-enhanced MRI (62).

4. Potential clinical applications of tFUS-BBBd

Based on promising safety data, FUS in combination with MBs has been used with the aim of administering a variety of therapeutic agents to the brain, and has started to show potential utilities in treating various diseases of the central nervous system.

Studies have successfully administered chemotherapies to deliver tumor-suppressing drugs such as doxorubicin in rats (46) and carboplatin in NHPs and humans (62) (using an implanted FUS transducer). These studies demonstrated tumor reduction without significant sonication-related damage. Cell-based therapy for cancer has also been sought after. For example, Natural killer (NK) cells have been delivered to HER-2 expressing human breast tumor cells, reducing the tumor size (59).

GFP-positive stem cells have been successfully delivered through the BBB to the left striatum and left hippocampus, presenting a potential use of FUS for stem-cell therapy to treat neurological diseases such as Parkinson's disease, traumatic brain injury, and stroke (56). Neurotropic factors with the capability of neuroregeneration, such as brain-derived neurotropic factor (66) and neurturin (74), have also been safely delivered through the BBB in mice.

For the potential treatment of Alzheimer's disease (AD), Jordão *et al.* delivered anti-Aβ antibodies to the brains of TgCRND8 mice (an AD animal model), and observed a significant reduction in number, size, and total surface area of Aβ plaques after four days (55). In a separate study, FUS-mediated BBBd was applied to the hippocampus of TgCRND8 mice, once every week for one month. Interestingly, without introducing any exogenous therapeutic agents, these repetitive, multi-session BBBd sessions have shown to decrease Aβ size and number and to improve performance on a memory task (Y-maze) (75). Although the mechanism behind this observation is not clear at this time, temporary disruption of BBB itself seems to have a powerful impact on improving AD-related symptoms, at least in the rodent model, and awaits further validation in humans.

Regional BBBd was shown to modulate the excitability of brain tissue in rats. Low pressure (*i.e.*, MI of 0.55 at 400 kHz) FUS to the primary somatosensory area (SI), combined with the introduction of MBs, resulted in short-term suppression of the EEG somatosensory evoked potentials (SSEP) lasting less than 1 h, whereas higher pressure (*i.e.*, MI of 0.8) given to the SI yielded prolonged (lasting 7 days) suppression of the SSEP amplitude and latency, suggesting suppressive effects on cortical excitability (60). The authors suggested a possible therapeutic application of this method for the suppression of epilepsy (60). On a similar note, it is plausible to conceive that tFUS-MB mediated BBBd can be used to temporarily increase the level of anti-epileptic drugs to the ictal locations for patients taking medication, but the serum level of medication may not be sufficient to suppress the ictal activity otherwise. More recently, Downs and colleagues opened the BBB in the putamen (unilaterally) in NHP performing visual-motor decision-making tasks, and showed that their decision making process improved (76). This observation led them to suggest that a similar technique can be used as a cognitive neural prosthetic device that may have a sustained and positive impact on performing complex cognitive tasks. Also, promising short-term anti-depressant effects have been observed from tFUS-MB administration on the hippocampus among rodents undergoing a forced-swim test (77).

Another emerging treatment possibility lies in non-invasive and focal acoustic transfection, whereby ultrasound waves can disrupt the lipid bilayer of the cell membrane for individual cells to deliver nucleic acids/genetic molecules into the cytoplasm. Conventionally, it involves using an ultrasound transducer with a fundamental frequency of over 150 MHz to deliver various sizes of macromolecules into the cell *in vitro* (78). If this technology could be safely combined with BBBd, it will hold the potential to introduce genetic materials to the brain *in vivo*. However, the increased level of absorption of the sound wave at the skull in this frequency range would cast additional challenges.

It is worthy to note that pulsed application of the FUS, when combined with tissue plasminogen activator (tPA) or similar thrombolytic agents, can be used to reduce the size of clots formed from spontaneous intracerebral hemorrhage (ICH) or ischemic stroke (79). The technique, widely known as sonothrombolysis, is currently under multi-center trials to examine its safety and efficacy (80). tFUS hardware can be readily adopted to serve this purpose, and the utility of MBs in this treatment setting await further investigations.

5. Summary and conclusions

For potential translations to human/clinical applications, multi-array MRgFUS systems or single-element FUS configurations can be used, and there are efforts from the industry to make these systems more available for research. Image-guidance in administering FUS to the targeted brain location is important, together with computer simulations to predict the location and the *in situ* pressure level. The combined use of CT and MRI for image-guidance is needed to identify the targeted brain location.

MBs should be given with a dose and timing in accordance with the vendor-suggested protocol for safety. The dominant method of MB administration is an IV bolus-injection, and FUS is given almost immediately after the injection. FF in a range of 200–700 kHz would be preferred in the case of human application to maximize the transcranial transmission of the acoustic energy. A TBD of 1–10 ms and PRF of ~1 Hz are applied for a duration of 1–2 min while the use of a longer TBD or a higher PRF does not seem to effectively increase the degree of BBBd.

The use of the lowest possible pressure that is enough to induce BBBd is important in initial translational investigations. A pressure level at a given FF that yields an MI of ~0.3–0.4 seems to be ideal, although an MI up to 0.7 may be acceptable based on literature. The use of the lowest possible acoustic pressure will also help to reduce the effects from possible formation of standing waves. Especially in the case of single-element FUS transducer configuration, the pressure level at the site of the standing wave is likely to be lower than that from the primary focus.

Repeated tFUS-BBBd sessions have been used in animal models while the gap between the sessions and number of sessions should be carefully characterized to ensure its safe use. Due to variability in effectiveness of BBBd according to individual neuroanatomy, monitoring of the presence and degree of the BBBd, with techniques such as dynamic contrast-enhanced MRI and cavitation detection, is desired to accompany the procedure.

tFUS-BBBd may ramify into a wide range of therapeutic applications, from drug to cell delivery, which may have a profound impact on the treatment of neurological disorders. Before this therapy can become widely available, further work is urgently warranted to probe the detailed safety parameters and efficacy of the procedure among NHPs and humans. Studies aiming to reveal detailed mechanisms behind the FUS-mediated BBBd also constitute major subjects of future investigations.

Acknowledgments

This study was supported by NIH (RO1 MH111763) to A. Cammalleri, P. Croce, W. Lee, K. Yoon, and S.S. Yoo.

References

1. Poon C, McMahon D, Hynynen K. Noninvasive and targeted delivery of therapeutics to the brain using focused ultrasound. Neuropharmacology. 2017; 120:20–37. [PubMed: 26907805]
2. Abbott NJ, Romero IA. Transporting therapeutics across the blood-brain barrier. Mol Med Today. 1996; 2(3):106–13. [PubMed: 8796867]
3. Engelhardt B, Sorokin L. The blood-brain and the blood-cerebrospinal fluid barriers: function and dysfunction. Semin Immunopathol. 2009; 31(4):497–511. [PubMed: 19779720]
4. Raja R, Rosenberg GA, Caprihan A. MRI measurements of blood-brain barrier function in dementia: A review of recent studies. Neuropharmacology. 2017
5. Pollak TA, Drndarski S, Stone JM, David AS, McGuire P, Abbott NJ. The blood-brain barrier in psychosis. Lancet Psychiatry. 2018; 5(1):79–92. [PubMed: 28781208]
6. Zlokovic BV. The blood-brain barrier in health and chronic neurodegenerative disorders. Neuron. 2008; 57(2):178–201. [PubMed: 18215617]
7. Dorovini-Zis K, Bowman PD, Betz AL, Goldstein GW. Hyperosmotic arabinose solutions open the tight junctions between brain capillary endothelial cells in tissue culture. Brain Res. 1984; 302(2):383–6. [PubMed: 6733518]
8. Kiyatkin EA, Sharma HS. Permeability of the blood-brain barrier depends on brain temperature. Neuroscience. 2009; 161(3):926–39. [PubMed: 19362131]
9. Suzuki T, Kohno H, Sakurada T, Tadano T, Kisara K. Intracranial injection of thyrotropin releasing hormone (TRH) suppresses starvation-induced feeding and drinking in rats. Pharmacol Biochem Behav. 1982; 17(2):249–53. [PubMed: 6813881]
10. Chen Y, Liu L. Modern methods for delivery of drugs across the blood-brain barrier. Adv Drug Deliv Rev. 2012; 64(7):640–65. [PubMed: 22154620]
11. Lee W, Lee SD, Park MY, et al. Image-guided focused ultrasound-mediated regional brain stimulation in sheep. Ultrasound Med Biol. 2016; 42(2):459–70. [PubMed: 26525652]
12. Hynynen K, McDannold N, Vykhodtseva N, Jolesz FA. Noninvasive MR imaging-guided focal opening of the blood-brain barrier in rabbits. Radiology. 2001; 220(3):640–6. [PubMed: 11526261]
13. Hu YZ, Zhu JA, Jiang YG, Hu B. Ultrasound microbubble contrast agents: application to therapy for peripheral vascular disease. Adv Ther. 2009; 26(4):425–34. [PubMed: 19381521]
14. Downs ME, Buch A, Sierra C, et al. Long-term safety of repeated blood-brain barrier opening via focused ultrasound with microbubbles in non-human primates performing a cognitive task. PLoS One. 2015; 10(5):e0125911. [PubMed: 25945493]
15. Wu SY, Sanchez CS, Samiotaki G, Buch A, Ferrera VP, Konofagou EE. Characterizing focused-ultrasound mediated drug delivery to the heterogeneous primate brain in vivo with acoustic monitoring. Sci Rep. 2016; 6:37094. [PubMed: 27853267]
16. Samiotaki G, Karakatsani ME, Buch A, et al. Pharmacokinetic analysis and drug delivery efficiency of the focused ultrasound-induced blood-brain barrier opening in non-human primates. Magn Reson Imaging. 2017; 37:273–81. [PubMed: 27916657]
17. Karakatsani MEM, Samiotaki GM, Downs ME, Ferrera VP, Konofagou EE. Targeting effects on the volume of the focused ultrasound-induced blood-brain barrier opening in nonhuman primates in vivo. IEEE Trans Ultrason Ferroelectr Freq Control. 2017; 64(5):798–810. [PubMed: 28320656]
18. Bader KB, Holland CK. Gauging the likelihood of stable cavitation from ultrasound contrast agents. Phys Med Biol. 2013; 58(1):127–44. [PubMed: 23221109]
19. Downs ME, Buch A, Karakatsani ME, Konofagou EE, Ferrera VP. Blood-brain barrier opening in behaving non-human primates via focused ultrasound with systemically administered microbubbles. Sci Rep. 2015; 5:15076. [PubMed: 26496829]

20. Chu PC, Chai WY, Tsai CH, Kang ST, Yeh CK, Liu HL. Focused ultrasound-induced blood-brain barrier opening: association with mechanical index and cavitation index analyzed by dynamic contrast-enhanced magnetic-resonance imaging. Sci Rep. 2016; 6:33264. [PubMed: 27630037]
21. Wu SY, Tung YS, Marquet F, et al. Transcranial cavitation detection in primates during blood-brain barrier opening--a performance assessment study. IEEE Trans Ultrason Ferroelectr Freq Control. 2014; 61(6):966–78. [PubMed: 24859660]
22. Tung YS, Vlachos F, Feshitan JA, Borden MA, Konofagou EE. The mechanism of interaction between focused ultrasound and microbubbles in blood-brain barrier opening in mice. J Acoust Soc Am. 2011; 130(5):3059–67. [PubMed: 22087933]
23. Hosseinkhah N, Goertz DE, Hynynen K. Microbubbles and blood-brain barrier opening: a numerical study on acoustic emissions and wall stress predictions. IEEE Trans Biomed Eng. 2015; 62(5):1293–304. [PubMed: 25546853]
24. Burgess A, Shah K, Hough O, Hynynen K. Focused ultrasound-mediated drug delivery through the blood-brain barrier. Expert Rev Neurother. 2015; 15(5):477–91. [PubMed: 25936845]
25. Lele PP. A simple method for production of trackless focal lesions with focused ultrasound: physical factors. J Physiol. 1962; 160(3):494–512. [PubMed: 14463953]
26. Khokhlova TD, Hwang JH. HIFU for palliative treatment of pancreatic cancer. J Gastrointest Oncol. 2011; 2(3):175–84. [PubMed: 22811848]
27. Hynynen K, Clement GT, McDannold N, et al. 500-element ultrasound phased array system for noninvasive focal surgery of the brain: a preliminary rabbit study with ex vivo human skulls. Magn Reson Med. 2004; 52(1):100–7. [PubMed: 15236372]
28. Bradley WG Jr. MR-guided focused ultrasound: a potentially disruptive technology. J Am Coll Radiol. 2009; 6(7):510–3. [PubMed: 19560068]
29. Maleke C, Konofagou EE. In vivo feasibility of real-time monitoring of focused ultrasound surgery (FUS) using harmonic motion imaging (HMI). IEEE Trans Biomed Eng. 2010; 57(1):7–11. [PubMed: 19643703]
30. Clement GT, White PJ, King RL, McDannold N, Hynynen K. A magnetic resonance imaging-compatible, large-scale array for trans-skull ultrasound surgery and therapy. J Ultrasound Med. 2005; 24(8):1117–25. [PubMed: 16040827]
31. Jing Y, Meral FC, Clement GT. Time-reversal transcranial ultrasound beam focusing using a k-space method. Phys Med Biol. 2012; 57(4):901–17. [PubMed: 22290477]
32. Martin E, Jeanmonod D, Morel A, Zadicario E, Werner B. High-intensity focused ultrasound for noninvasive functional neurosurgery. Ann Neurol. 2009; 66(6):858–61. [PubMed: 20033983]
33. McDannold N, Clement GT, Black P, Jolesz F, Hynynen K. Transcranial magnetic resonance imaging- guided focused ultrasound surgery of brain tumors: initial findings in 3 patients. Neurosurgery. 2010; 66(2):323–32. [PubMed: 20087132]
34. Lee W, Kim H, Jung Y, Song I-U, Chung YA, Yoo S-S. Image-guided transcranial focused ultrasound stimulates human primary somatosensory cortex. Sci Rep. 2015; 5:8743. [PubMed: 25735418]
35. Yoo SS, Bystritsky A, Lee JH, et al. Focused ultrasound modulates region-specific brain activity. Neuroimage. 2011; 56(3):1267–75. [PubMed: 21354315]
36. Lee W, Kim S, Kim B, et al. Non-invasive transmission of sensorimotor information in humans using an EEG/focused ultrasound brain-to-brain interface. PLoS One. 2017; 12(6):e0178476. [PubMed: 28598972]
37. Lee W, Chung YA, Jung Y, Song IU, Yoo SS. Simultaneous acoustic stimulation of human primary and secondary somatosensory cortices using transcranial focused ultrasound. BMC Neurosci. 2016; 17(1):68. [PubMed: 27784293]
38. Kaye EA, Chen J, Pauly KB. Rapid MR-ARFI method for focal spot localization during focused ultrasound therapy. Magn Reson Med. 2011; 65(3):738–43. [PubMed: 21337406]
39. Schwenke M, Strehlow J, Haase S, et al. An integrated model-based software for FUS in moving abdominal organs. Int J Hyperthermia. 2015; 31:240–50. [PubMed: 25786982]
40. White PJ, Clement GT, Hynynen K. Longitudinal and shear mode ultrasound propagation in human skull bone. Ultrasound Med Biol. 2006; 32(7):1085–96. [PubMed: 16829322]

41. Deffieux T, Konofagou EE. Numerical study of a simple transcranial focused ultrasound system applied to blood-brain barrier opening. IEEE Trans Ultrason Ferroelectr Freq Control. 2010; 57(12):2637–53. [PubMed: 21156360]
42. McDannold N, Vykhodtseva N, Hynynen K. Blood-brain barrier disruption induced by focused ultrasound and circulating preformed microbubbles appears to be characterized by the mechanical index. Ultrasound Med Biol. 2008; 34(5):834–40. [PubMed: 18207311]
43. Kaufman JJ, Luo G, Siffert RS. Ultrasound simulation in bone. IEEE Trans Ultrason Ferroelectr Freq Control. 2008; 55(6):1205–18. [PubMed: 18599409]
44. Treeby BE, Cox BT. k-Wave: MATLAB toolbox for the simulation and reconstruction of photoacoustic wave fields. J Biomed Opt. 2010; 15(2):021314. [PubMed: 20459236]
45. Hynynen K, McDannold N, Sheikov NA, Jolesz FA, Vykhodtseva N. Local and reversible blood-brain barrier disruption by noninvasive focused ultrasound at frequencies suitable for trans-skull sonications. Neuroimage. 2005; 24(1):12–20. [PubMed: 15588592]
46. Treat LH, McDannold N, Vykhodtseva N, Zhang Y, Tam K, Hynynen K. Targeted delivery of doxorubicin to the rat brain at therapeutic levels using MRI-guided focused ultrasound. Int J Cancer. 2007; 121(4):901–7. [PubMed: 17437269]
47. McDannold N, Arvanitis CD, Vykhodtseva N, Livingstone MS. Temporary disruption of the blood-brain barrier by use of ultrasound and microbubbles: safety and efficacy evaluation in rhesus macaques. Cancer Res. 2012; 72(14):3652–63. [PubMed: 22552291]
48. Kovacs ZI, Kim S, Jikaria N, et al. Disrupting the blood-brain barrier by focused ultrasound induces sterile inflammation. Proc Natl Acad Sci U S A. 2017; 114(1):E75–E84. [PubMed: 27994152]
49. O'Reilly MA, Waspe AC, Ganguly M, Hynynen K. Focused-ultrasound disruption of the blood-brain barrier using closely-timed short pulses: influence of sonication parameters and injection rate. Ultrasound Med Biol. 2011; 37(4):587–94. [PubMed: 21376455]
50. McDannold N, Vykhodtseva N, Hynynen K. Effects of acoustic parameters and ultrasound contrast agent dose on focused-ultrasound induced blood-brain barrier disruption. Ultrasound Med Biol. 2008; 34(6):930–7. [PubMed: 18294757]
51. Hynynen K, McDannold N, Vykhodtseva N, et al. Focal disruption of the blood-brain barrier due to 260-kHz ultrasound bursts: a method for molecular imaging and targeted drug delivery. J Neurosurg. 2006; 105(3):445–54. [PubMed: 16961141]
52. Liu HL, Wai YY, Chen WS, et al. Hemorrhage detection during focused-ultrasound induced blood-brain-barrier opening by using susceptibility-weighted magnetic resonance imaging. Ultrasound Med Biol. 2008; 34(4):598–606. [PubMed: 18313204]
53. Yang FY, Liu SH, Ho FM, Chang CH. Effect of ultrasound contrast agent dose on the duration of focused-ultrasound-induced blood-brain barrier disruption. J Acoust Soc Am. 2009; 126(6):3344–9. [PubMed: 20000948]
54. Liu HL, Hua MY, Chen PY, et al. Blood-brain barrier disruption with focused ultrasound enhances delivery of chemotherapeutic drugs for glioblastoma treatment. Radiology. 2010; 255(2):415–25. [PubMed: 20413754]
55. Jordao JF, Ayala-Grosso CA, Markham K, et al. Antibodies targeted to the brain with image-guided focused ultrasound reduces amyloid-beta plaque load in the TgCRND8 mouse model of Alzheimer's disease. PLoS One. 2010; 5(5):e10549. [PubMed: 20485502]
56. Burgess A, Ayala-Grosso CA, Ganguly M, Jordao JF, Aubert I, Hynynen K. Targeted delivery of neural stem cells to the brain using MRI-guided focused ultrasound to disrupt the blood-brain barrier. PLoS One. 2011; 6(11):e27877. [PubMed: 22114718]
57. McDannold N, Zhang Y, Vykhodtseva N. Blood-brain barrier disruption and vascular damage induced by ultrasound bursts combined with microbubbles can be influenced by choice of anesthesia protocol. Ultrasound Med Biol. 2011; 37(8):1259–70. [PubMed: 21645965]
58. Yang FY, Lin YS, Kang KH, Chao TK. Reversible blood-brain barrier disruption by repeated transcranial focused ultrasound allows enhanced extravasation. J Control Release. 2011; 150(1):111–6. [PubMed: 21070825]
59. Alkins R, Burgess A, Ganguly M, et al. Focused ultrasound delivers targeted immune cells to metastatic brain tumors. Cancer Res. 2013; 73(6):1892–9. [PubMed: 23302230]

60. Chu PC, Liu HL, Lai HY, Lin CY, Tsai HC, Pei YC. Neuromodulation accompanying focused ultrasound-induced blood-brain barrier opening. Sci Rep. 2015; 5:15477. [PubMed: 26490653]
61. Lin CY, Hsieh HY, Pitt WG, et al. Focused ultrasound-induced blood-brain barrier opening for non-viral, non-invasive, and targeted gene delivery. J Control Release. 2015; 212:1–9. [PubMed: 26071631]
62. Goldwirt L, Canney M, Horodyckid C, et al. Enhanced brain distribution of carboplatin in a primate model after blood-brain barrier disruption using an implantable ultrasound device. Cancer Chemother Pharmacol. 2016; 77(1):211–6. [PubMed: 26645405]
63. Kobus T, Vykhodtseva N, Pilatou M, Zhang Y, McDannold N. Safety validation of repeated blood-brain barrier disruption using focused ultrasound. Ultrasound Med Biol. 2016; 42(2):481–92. [PubMed: 26617243]
64. Carpentier A, Canney M, Vignot A, et al. Clinical trial of blood-brain barrier disruption by pulsed ultrasound. Sci Transl Med. 2016; 8(343):343re2.
65. Baseri B, Choi JJ, Tung YS, Konofagou EE. Multi-modality safety assessment of blood-brain barrier opening using focused ultrasound and definity microbubbles: a short-term study. Ultrasound Med Biol. 2010; 36(9):1445–59. [PubMed: 20800172]
66. Baseri B, Choi JJ, Deffieux T, et al. Activation of signaling pathways following localized delivery of systemically administered neurotrophic factors across the blood-brain barrier using focused ultrasound and microbubbles. Phys Med Biol. 2012; 57(7):N65–81. [PubMed: 22407323]
67. Horodyckid C, Canney M, Vignot A, et al. Safe long-term repeated disruption of the blood-brain barrier using an implantable ultrasound device: a multiparametric study in a primate model. J Neurosurg. 2017; 126(4):1351–61. [PubMed: 27285538]
68. Younan Y, Deffieux T, Larrat B, Fink M, Tanter M, Aubry JF. Influence of the pressure field distribution in transcranial ultrasonic neurostimulation. Med Phys. 2013; 40(8):082902. [PubMed: 23927357]
69. Kim YB, Bae KH, Yoo SS, Park TG, Park H. Positive contrast visualization for cellular magnetic resonance imaging using susceptibility-weighted echo-time encoding. Magn Reson Imaging. 2009; 27(5):601–10. [PubMed: 19106021]
70. Yoo SS, Gil Choi B, Han JY, Hee Kim H. Independent component analysis for the examination of dynamic contrast-enhanced breast magnetic resonance imaging data: preliminary study. Invest Radiol. 2002; 37(12):647–54. [PubMed: 12446997]
71. Heye AK, Culling RD, Valdes Hernandez Mdel C, Thrippleton MJ, Wardlaw JM. Assessment of blood-brain barrier disruption using dynamic contrast-enhanced MRI. A systematic review. Neuroimage Clin. 2014; 6:262–74. [PubMed: 25379439]
72. Hynynen K. Ultrasound for drug and gene delivery to the brain. Adv Drug Deliv Rev. 2008; 60(10):1209–17. [PubMed: 18486271]
73. Nhan T, Burgess A, Cho EE, Stefanovic B, Lilge L, Hynynen K. Drug delivery to the brain by focused ultrasound induced blood-brain barrier disruption: quantitative evaluation of enhanced permeability of cerebral vasculature using two-photon microscopy. J Control Release. 2013; 172(1):274–80. [PubMed: 24008151]
74. Samiotaki G, Acosta C, Wang S, Konofagou EE. Enhanced delivery and bioactivity of the neurturin neurotrophic factor through focused ultrasound-mediated blood--brain barrier opening in vivo. J Cereb Blood Flow Metab. 2015; 35(4):611–22. [PubMed: 25586140]
75. Burgess A, Dubey S, Yeung S, et al. Alzheimer disease in a mouse model: MR imaging-guided focused ultrasound targeted to the hippocampus opens the blood-brain barrier and improves pathologic abnormalities and behavior. Radiology. 2014; 273(3):736–45. [PubMed: 25222068]
76. Downs ME, Teichert T, Buch A, et al. Toward a cognitive neural prosthesis using focused ultrasound. Front Neurosci. 2017; 11:607. [PubMed: 29187808]
77. Mooney SJ, Nobrega JN, Levitt AJ, Hynynen K. Antidepressant effects of focused ultrasound induced blood-brain-barrier opening. Behav Brain Res. 2018; 342:57–61. [PubMed: 29326057]
78. Yoon S, Kim MG, Chiu CT, et al. Direct and sustained intracellular delivery of exogenous molecules using acoustic-transfection with high frequency ultrasound. Sci Rep. 2016; 6:20477. [PubMed: 26843283]

79. Papadopoulos N, Damianou C. In vitro evaluation of focused ultrasound-enhanced TNK-tissue plasminogen activator-mediated thrombolysis. J Stroke Cerebrovasc Dis. 2016; 25(8):1864–77. [PubMed: 27156900]

80. Ebben HP, Nederhoed JH, Lely RJ, Wisselink W, Yeung K, collaborators M. Microbubbles and ultrasound-accelerated thrombolysis (MUST) for peripheral arterial occlusions: protocol for a phase II single-arm trial. BMJ Open. 2017; 7(8):e014365.

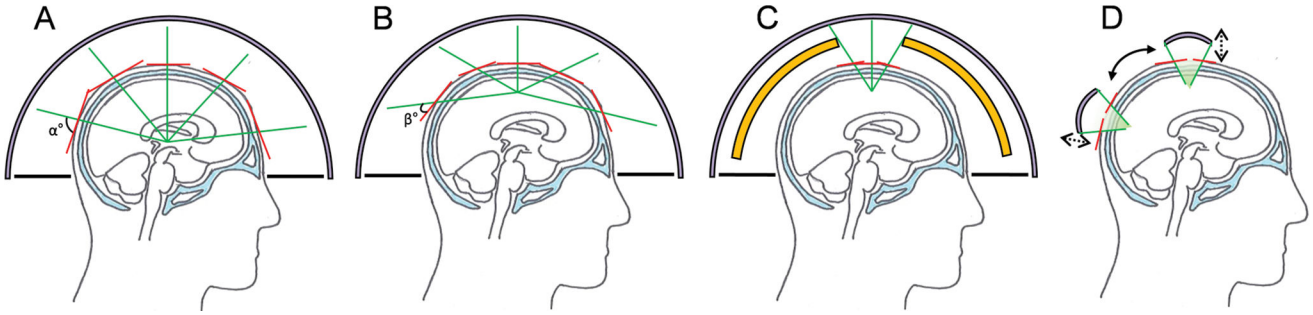

Fig. 1.

Illustration of different modes of tFUS configurations (human example). (A) Sonication of deep brain structures using a multi-element transducer. Red lines indicate the surface tangential to the skull with respect to the incident sonication beam originating from each element (in green line), (B) Sonication of cortical area near the skull surface. (C) Beam selection (in green line) by blocking (in yellow) or (D) use of single-element FUS transducer under the image-guidance to track the location of the transducer with respect to the head.

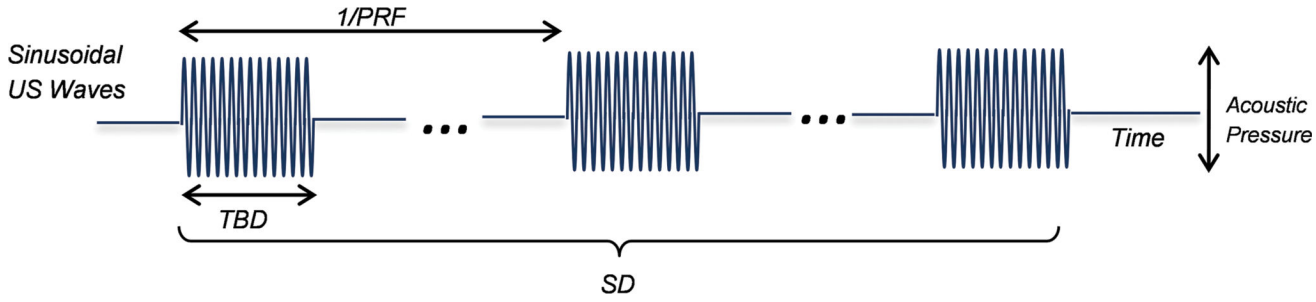

Fig. 2.
Illustration for the definition of sonication parameters used.

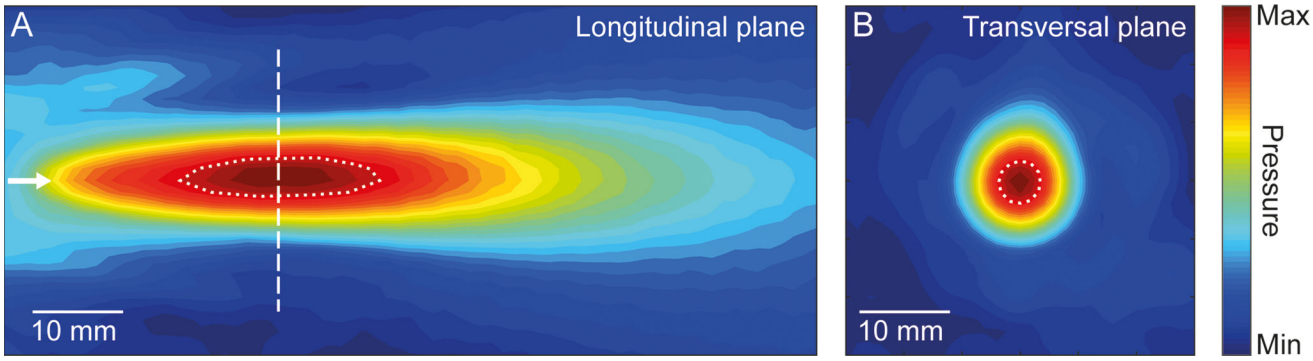

Fig. 3.

Spatial map of acoustic pressure distribution obtained from a single-element FUS transducer operating at 250 kHz, with an F-number of 1.2. The map was obtained using a needle hydrophone mounted to a robotic stage that measured acoustic pressure originating from the transducer, and was pseudo-colored to represent its relative magnitude. (A) Pressure distribution longitudinal to the wave propagation (a white arrow indicates the direction of propagation). (B) Pressure distribution in the transverse plane at the focal region (dashed line from the panel A). The dotted profiles indicate areas with ≥ 90% of the maximum pressure level.

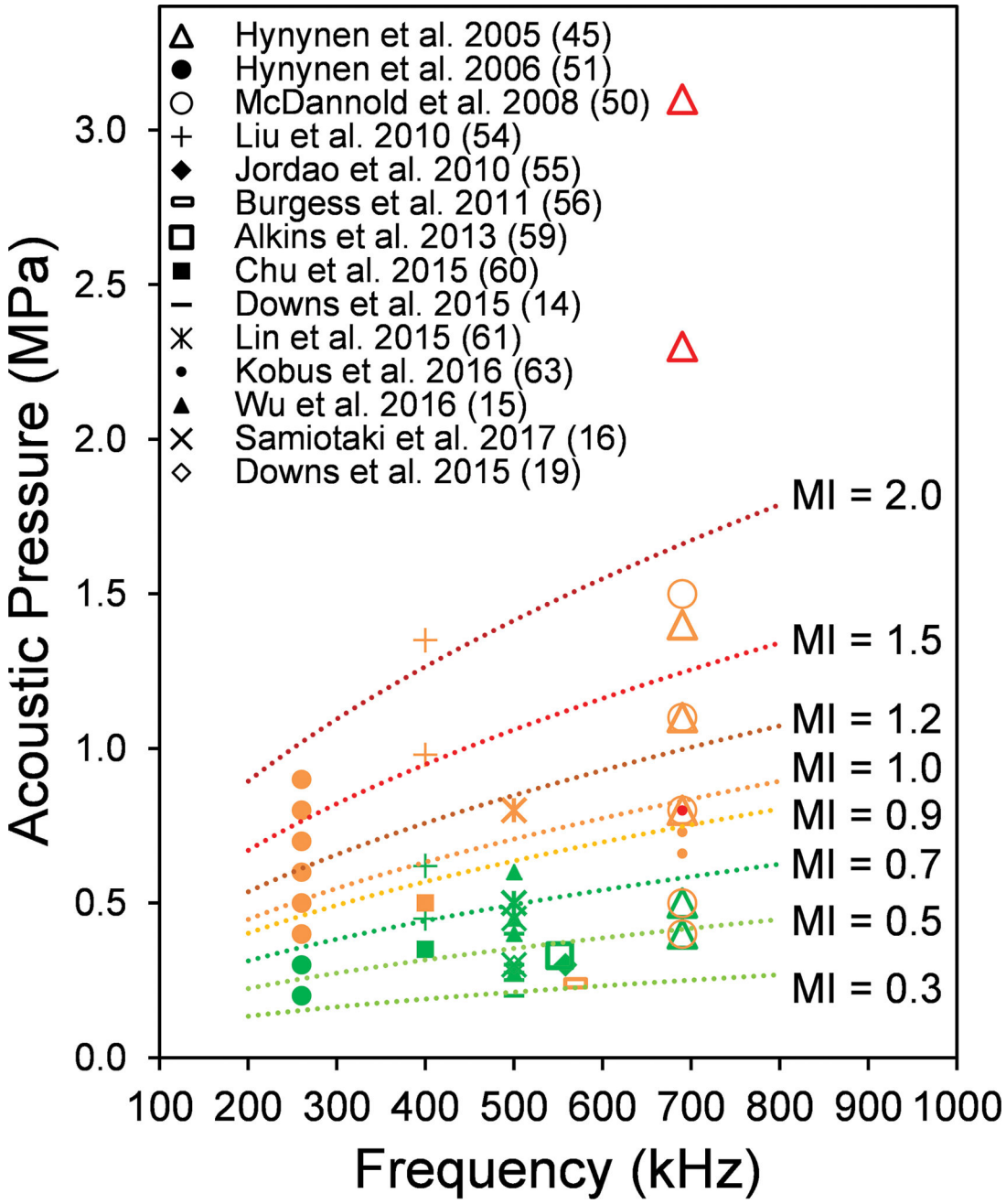

Fig. 4.

Frequencies and acoustic pressures previously used for successful BBBd using FUS (across different animal species) and the degree of observed vascular/tissue damage, with different MI values overlaid. For the given marker, green indicates successful BBBd without damage, orange indicates the presence of minor damage, whereby the red indicates extensive damage to the brain. Only the results using a FF under 1 MHz were included (based on n = 14 papers published).

Table 1

Overview of FUS studies for BBBd (FF: Fundamental Frequency, TBD: Tone burst duration, SD: Sonication duration, PRF: Pulse repetition frequency, MI: Mechanical Index)

Year	Reference	Animal/ Species	Sonication Target	Contrast Agent	FF (kHz)	TBD (ms)	SD (s)	PRF (Hz)	Pressure (MPa)	MI	Success? (Y or N)	Damage?
2005	Hynynen K, McDannold N, Sheikov NA, et al. (45)	New Zealand (NZ) Rabbits (3–4 kg; M)	1–6 locations in grey matter with center of focal spot 10 mm deep	Optison (0.05 mL/kg)	690	10	20	1	0	0.0	N	None
					690	10	20	1	0.4–0.5	0.5–0.6	Y	One or a few small erythrocyte extravasations
					690	10	20	1	0.8–1.4	1.0–1.7	Y	Minor—Petechial hemorrhages; mild damage to the brain parenchyma
					690	10	20	1	2.3–3.1	2.8–3.7	Y	High—Hemorrhagic or non-hemorrhagic local lesions
2006	Hynynen K, McDannold N, Vykhodtseva N, et al. (51)	NZ Rabbits (3–4 kg; M)	1–4 locations in grey matter with center of focal spot 10 mm deep	Optison (0.05 mL/kg)	260	10	20	1	0–0.1	0.0–0.2	N	None
					260	10	20	1	0.2–0.3	0.4–0.6	Y	None
					260	10	20	1	0.4–0.9	0.8–1.8	Y	Minor *
2007	Treat LH, McDannold N, Vykhodtseva N, et al. (46)	Sprague-Dawley Rats (300–400 g)	Thalamus, hippocampus, superior colliculus, caudate, putamen	Optison (0.1 mL/kg)	1500–1700	10	30–120	1	0.36–2.5	0.3–2.0	Y	Minor—A few extravasated erythrocytes, no necrotic lesions
2008	McDannold N, Vykhodtseva N, Hynynen K, et al. (50)	NZ Rabbits (4 kg; M)	Thalamus (1 cm deep, 3 mm lateral to the midline)	Optison (50 μg/kg)	690	0.1	20	1	0.4–0.5	0.5–0.6	Y	Minor vascular damage—Extravasations (one or a few isolated erythrocytes to clusters of cells)
					690	0.1	20	1	0.8	1.0	Y	
					690	0.1	20	1	1.1–1.5	1.3–1.8	Y	
					690	1	20	1	0.4	0.5	Y	
					690	1	20	1	0.5	0.6	Y	
					690	1	20	1	0.8–1.1	1.0–1.3	Y	
					690	10	20	1	0.5	0.6	Y	
					690	10	20	0.5–5	0.5	0.6	Y	
				Optison (100 μg/kg)	690	10	20	1	0.5	0.6	Y	
				Optison (250 μg/kg)	690	10	20	1	0.5	0.6	Y	
2008	Liu HL, Wai YY, Chen WS, et al. (52)	Sprague-Dawley Rats (M)	Anterior area (not specified)	SonoVue (0.025 mL/kg)	1500	10	30	1	0.55–1.1	0.4–0.9	Y	No hemorrhage or tissue damage
					1500	10	30	1	1.9–3.47	1.6–2.8	Y	Occasional or groups of erythrocyte extravasations
					1500	10	30	1	4.9	4.0	Y	Hemorrhage with vacuolated cells, necrotic cell death, and extensive tissue damage
2008	McDannold N, Vykhodtseva N, Hynynen K. (42)	NZ Rabbits	Thalamus (1 cm deep & ~2–3 mm from the midline)	Optison (50 μL/kg)	2040	10	20	1	0.3–2.3	0.2–1.6	Y	Minor vascular damage

Year	Reference	Animal/ Species	Sonication Target	Contrast Agent	FF (kHz)	TBD (ms)	SD (s)	PRF (Hz)	Pressure (MPa)	MI	Success? (Y or N)	Damage?
2009	Yang FY. (53)	Sprague-Dawley Rats (280–350 g)	Right hemisphere (3.5 mm posterior & 2.5 mm lateral to the bregma & 5.7 mm below skull surface)	SonoVue (150 μg/kg)	1000	50	60	1	Acoustic power was given (1.43 W)	N/A	Y	No hemorrhage
				SonoVue (300–450 μg/kg)	1000	50	60	1	Acoustic power was given (1.43 W)	N/A	Y	Hemorrhage
2010	Baseri B, Choi JJ, Tung YS, et al. (65)	CB57L/6 Mice (18–31 g; M)	Thalamus, hippocampal fissure (dentate gyrus and CA3)	Definity (0.05 μg/kg)	1525	20	30	10	0.15	0.1	N	N/A
					1525	20	30	10	0.3	0.2	Y	Little or no tissue effects
					1525	20	30	10	0.46	0.4	Y	No detectable hemorrhage, but increased extravasted red blood cells, dark neurons, and microvacuolations
					1525	20	30	10	0.61	0.5	Y	No detectable hemorrhage, tissue damage in 66%of samples
					1525	20	30	10	0.75	0.6	Y	No detectable hemorrhage, tissue damage in 77%of samples
					1525	20	30	10	0.9	0.7	Y	No detectable hemorrhage
					1525	20	30	10	0.98	0.8	Y	Large scale hemorrhage and extensive tissue damage
2010	Liu HL, Hua MY, Chen PY, et al. (54)	Sprague- Dawley Rats (250–300 g; M)	Striatum	SonoVue (2.5 μg/kg)	400	10	30	1	0.45	0.7	N	None
					400	10	30	1	0.48–0.62	0.7–1.0	Y	None
					400	10	30	1	0.98–1.35	1.5–2.1	Y	Intracerebral hemorrhage
2010	Jordão JF, Ayala-Grosso CA, Markham K, et al. (55)	TgCRND8 Mice	Right hemisphere (4 spots 1.5 mm apart)	Definity (160 μg/kg)	558	10	120	1	0.3	0.4	Y	None
2011	Burgess A, Ayala-Grosso CA, Ganguly M, et al. (56)	Sprague-Dawley Rats (200–250 g)	Left striatum	Definity (0.2 mg/kg)	558	10	120	1	0.24	0.3	Y	Minimal—Extravasated erythrocytes in tissue at sight of sonication
2011	McDannold N, Zhang Y, Vykhodtseva N. (57)	Rats (250 g; M)	Thalamus, putamen	Definity (10 μg/kg)	532	10	60	1	0.13–0.3	0.2–0.4	Y	Extensive extravasations at pressures ≥0.2 MPa
2011	Yang FY, Lin YS, Kang KH, Chao TK. (58)	Sprague-Dawley Rats (280–350 g; M)	Right hemisphere	SonoVue (150 μg/kg)	1000	50	0	1	0.9	0.9	N	Some inflammatory cell aggregation, no vacuolation with a single sonication, some vacuolation and degeneration in brains sonicated twice
					1000	50	20–30	1	0.9	0.9	Y	
					1000	50	40–60	1	0.9	0.9	Y	
2012	McDannold N, Arvanitis CD, Vykhodtseva N, et al. (47)	Rhesus Macaques (5–12 kg)	Hippocampus/LGN, primary visual cortex , cingulate cortex, and amygdala	Definity (10 or 20 μg/kg)	220	10	70, 150	0.28–1.1	0.1–0.7	0.2– 1.5	Y	Tissue damage at 0.3 MPa (50% probability)
												Severe parenchymal & vascular damages at 0.44–0.7 MPa

Year	Reference	Animal/ Species	Sonication Target	Contrast Agent	FF (kHz)	TBD (ms)	SD (s)	PRF (Hz)	Pressure (MPa)	MI	Success? (Y or N)	Damage?
			Various locations including thalamus, putamen, and hippocampus		220	10	70, 150	0.28–1.1	0.1–0.7	0.2– 1.5	Y	Tissue damage at 0.3 MPa (50% probability)
												Severe parenchymal & vascular damages at 0.444–0.7 MPa
2013	Alkins R, Burgess A, Ganguly M, et al. (59)	Nude Rats (250–300 g; M)	Left frontal striatum	Definity (0.2 mL/kg)	551.5	10	120	1	0.33	0.4	Y	None
2015	Chu PC, Liu HL, Lai HY, et al. (60)	Sprague- Dawley Rats (250–300 g; M)	Left primary somatosensory cortex	SonoVue (0.1 mL/kg)	400	10	120	1	0.2	0.3	N	None
					400	10	120	1	0.35	0.6	Y	None
					400	10	120	1	0.5	0.8	Y	Erythrocytes extravasations
2015	Downs ME, Buch A, Sierra C, et al. (14)	Macaques (5–9 kg; M)	Caudate, putamen	Made in house	500	10	120	2	0.2–0.4	0.3–0.6	Y	None
2015	Lin CY, Hsieh HY, Pitt WG, et al. (61)	Balb/c mice (25 g; M)	Left hemisphere	SonoVue (4 μg/kg)	500	10	60	1	0.5	0.7	Y	None
					500	10	60	1	0.3	0.4	N	None
					500	10	60	1	0.8	1.1	Y	Hemorrhage damage
2015	Downs ME, Buch A, Karakatsani ME, et al. (19)	Macaques (5.3, 5.6 kg; M)	Caudate, putamen, thalamus	Made in house	500	10	120	2	0.3	0.4	Y	None
2016	Goldwirt L, Canney M, Horodyckid C, et al. (62)	Papio Anubis Baboon (27 kg)	Motor area to skull surface	SonoVue (0.1 cc/kg)	1050	23.2	134	1	0.9	0.9	Y	None
2016	Kovacs ZI, Kim S, Jikaria N, et al. (48)	Sprague-Dawley Rats (8–10 wk old; F)	Left cortex, striatum	Optison (100 μL)	589.6	10	120	1	0.3	0.4	Y	Sterile inflammatory response (lasted 24 h)
2016	Kobus T, Vykhodtseva N, Pilatou M, et al. (63)	Sprague-Dawley Rats	Right hemisphere (3 locations, 1 mm apart)	Definity (10 μg/kg)	690	10	60	1	0.66	0.8	Y	Microscars
					690	10	60	1	0.73	0.9	Y	Scattered micro-hemorrhaging
					690	10	60	1	0.8	1.0	Y	Hemorrhages
2016	Wu SY, Sanchez CS, Samiotaki G, et al. (15)	Rhesus Macaques (M)	Caudate, putamen	Made in house (4–5 μm in diameter)	500	10	120	2	0.28–0.6	0.4–0.8	Y	None
2016	Carpentier A, Canney M, Vignot A, et al. (64)	Human	Tumor (1 cm in diameter)	SonoVue (4.8 mL/kg)	1050	23.8	150	1	0.5–0.65	0.5–0.6	N	None
				SonoVue (4.8–8.1 mL/kg)	1050	23.8	150	1	0.8–1.1	0.8–1.1	Y	None
2017	Karakatsani ME, Samiotaki GM, Downs ME, et al. (17)	Rhesus Macaques & Marmoset	Caudate, putamen	Made in House (4–5 μm in diameter)	500	10	120	2	0.25–0.6	0.4–0.8	Y	None
2017	Samiotaki G, Karakatsani ME, Buch A, et al. (16)	Rhesus Macaques (10 kg; M)	Caudate, putamen	Made in House (4–5 μm in diameter)	500	10	120	2	0.3–0.45	0.4–0.6	Y	None
2017	Horodyckid C, Canney M, Vignot A, et al. (67)	Baboons & Macaque (8–27kg)	Motor cortex	SonoVue (0.1 mL/kg)	1050	23.2	120	1	0.6–0.8	0.6–0.8	Y	None

*At 0.4 MPa, 80% of locations showed vascular effects ranging from a few scattered erythrocytes to multiple petechial extravasations. Mild damage to the parenchyma, no area with multiple ischemic or apoptotic neurons was observed.